Geophysical Research Letters

RESEARCH LETTER
10.1029/2020GL091615

Key Points:

- A universal indicator for air flow vertical decoupling is derived
- The indicator enables analytical estimation of flow decoupling dependency on height, stratification, and leaf area index
- The indicator should be applicable at most flux measurement sites, since it relies only on basic micrometeorological measurements

Supporting Information:

- Supporting Information S1

Correspondence to:
O. Peltola,
olli.peltola@fmi.fi

Citation:
Peltola, O., Lapo, K., & Thomas, C. K. (2021). A physics-based universal indicator for vertical decoupling and mixing across canopies architectures and dynamic stabilities. *Geophysical Research Letters*, *48*, e2020GL091615. https://doi.org/10.1029/2020GL091615

Received 10 NOV 2020
Accepted 30 JAN 2021

A Physics-Based Universal Indicator for Vertical Decoupling and Mixing Across Canopies Architectures and Dynamic Stabilities

O. Peltola[1], K. Lapo[2,3], and C. K. Thomas[2,3]

[1]Climate Research Programme, Finnish Meteorological Institute, Helsinki, Finland, [2]Micrometeorology Group, University of Bayreuth, Bayreuth, Germany, [3]Bayreuth Center for Ecology and Environmental Research (BayCEER), University of Bayreuth, Bayreuth, Germany

Abstract Air flows may be decoupled from the underlying surface either due to strong stratification of air or due to canopy drag suppressing cross-canopy mixing. During decoupling, turbulent fluxes vary with height and hence identification of decoupled periods is crucial for the estimation of surface fluxes with the eddy covariance (EC) technique and computation of ecosystem-scale carbon, heat, and water budgets. A new indicator for identifying the decoupled periods is derived using forces (buoyancy and canopy drag) hindering movement of a downward propagating air parcel. This approach improves over the existing methods since (1) changes in forces hindering the coupling are accounted for, and (2) it is based on first principles and not on ad hoc empirical correlations. The applicability of the method is demonstrated at two contrasting EC sites (flat open terrain, boreal forest) and should be applicable also at other EC sites above diverse ecosystems (from grasslands to dense forests).

Plain Language Summary Air flows may be disconnected (i.e., decoupled) from the surface below, meaning that the properties of the flow (e.g., wind speed, temperature, concentrations of gases, pollutants, or particles) do not react to changes at the surface. During these periods, air temperatures near the ground decrease and concentrations of gases, pollutants and particles increase significantly since they are not transported upwards, but rather stay close to the ground. These decoupling periods can take place when the air is strongly stratified (e.g., clear sky, weak wind nights) or thick forest canopies inhibit air mixing. Controls on flow decoupling are poorly understood, yet the phenomenon has significance for scientific monitoring networks and also for the general public due to its connection for example, to air quality and frost formation. In this study, we derive a new indicator for flow decoupling, demonstrate its applicability at two measurement sites and discuss variables controlling decoupling in the light of this new indicator.

1. Introduction

Understanding of air flows and mixing in the very stable boundary layer (vSBL) often observed for example, during clear sky, weak wind nights persists to be incomplete (Mahrt, 2014). This issue poses problems for all scientific studies enquiring into surface-atmosphere interactions including mass and energy budgets, since they rely on turbulence observations or boundary layer theories, both of which tend to fail under strong stratification.

The stable stratification, resulting from surface cooling via radiative heat loss, suppresses vertical turbulent mixing. Under strong enough stratification and weak turbulence production via wind shear, the turbulent eddies become detached from the surface, that is, they are not coupled to the surface. This results in so-called "z-less" scaling of turbulence statistics (Nieuwstadt, 1984), meaning that distance from the surface is no longer a governing length scale (Grachev et al., 2013; Li et al., 2016; Sorbjan, 2006; Sorbjan & Balsley, 2008). As eddies detach from the surface, they lose their immediate connection to the exchange of momentum, heat and gases at the surface resulting in vertical variability of turbulent flux of these constituents with height (Mahrt et al., 2018).

Vertical variability of turbulent flux in this decoupled flow regime poses a severe problem for the global eddy covariance (EC) flux measurement network (FLUXNET; Baldocchi, 2014) and a clear solution for the

problem is lacking (Aubinet et al., 2010). FLUXNET is the main observational tool to study global terrestrial carbon and water cycles and the accuracy of the network largely hinges upon proper identification of decoupled and coupled flow regimes. Only in latter case EC observations integrate over all sinks and sources and thus can provide biophysically meaningful estimates of carbon, water and heat budgets. Accurate estimates of terrestrial carbon cycle are sorely needed for constraining the global carbon budget (Friedlingstein et al., 2019).

Commonly the friction velocity (u_*) is used to identify decoupled periods from continuous flux time series, albeit this approach is known to be flawed, in particular at sites with dense canopies (Acevedo et al., 2009; Freundorfer et al., 2019; Jocher et al., 2018; Thomas & Foken, 2007a; Thomas et al., 2013). Various other metrics have been used to identify the weakly stable from the very stable flow regime (Mahrt et al., 1998; Sun et al., 2012; Williams et al., 2013). However, they all rely on uncertain site-specific threshold values and were developed for open areas and hence their applicability to forested regions remains unclear (Freundorfer et al., 2019). Canopy flows differ markedly from the air flows above short vegetation, due to prevalence of coherent flow structures (Finnigan, 2000; Finnigan et al., 2009; Raupach et al., 1996; Thomas & Foken, 2007b) and the momentum sink for the air flow caused by canopy drag. The latter can cause the air flows above forests to be decoupled from the forest floor also during daytime (Jocher et al, 2017, 2018; Kruijt et al., 2000; Santana et al., 2018; Thomas et al., 2013).

In this study, we aim to advance the mechanistic understanding of flow coupling to the surface, in particular in the presence of emergent vegetation and/or strong stratification. Here we define a "weakly stable regime" to be governed by eddies which communicate with the surface (z-scaling applies), whereas in the "strongly stable regime" the large wall-attached eddies are not prevalent. A simple air parcel technique is used to evaluate the flow coupling to the surface. A novel metric is proposed to identify the flow regime and variables controlling the decoupling are discussed. The metric may be applied across the entire gradients from short canopies (e.g., grass, crop, and snow) to dense tall forests and hence applicable at most flux sites monitoring ecosystem-atmosphere interactions.

2. Theory

Coupled air layers are defined in this study as follows: air parcels travel between the coupled air layers and facilitate the exchange of heat, mass and momentum between the layers. Therefore, there is a direct interaction between the layers. In contrast, air parcels do not travel between decoupled air layers and hence there is no direct thermodynamic interaction between the layers (albeit waves can still transport momentum). When considering coupling of air layer at height z above ground with the surface, based on this definition there need to be air parcels that can traverse the vertical distance of z. This concurs with the notion that in coupled situations large wall-attached eddies that scale with z dominate the flow (Lan et al., 2018; Sun et al., 2012, 2020). Note that the concept proposed below is based on first principles and does not assume for example, the surface layer similarity theories to be valid. Similar air parcel approaches have been used (e.g., Mahrt, 1979; Mahrt et al., 2012; Sorbjan, 2006; Sorbjan & Balsley, 2008; Zeeman et al., 2013) to derive e.g. relevant length scales in the stable boundary layer, here it is used in canopy flows to examine the coupled air layer.

Movement of downward moving air parcels at the canopy height (h) is hindered by any opposing forces which include canopy drag caused by the foliage (e.g., Cescatti & Marcolla, 2004; Poggi, Katul et al, 2004a; Watanabe, 2004) and buoyancy force inflicted by stably stratified air layers. In order to reach the ground, an air parcels kinetic energy must match or exceed the work performed against the hindering forces. Based on this a critical speed ($w_{e,\mathrm{crit}}$) for the air parcel can be derived (see supporting information):

$$w_{e,crit} = -\gamma \hat{c}_d \,\mathrm{LAI} U_h - \sqrt{\gamma^2 \hat{c}_d{}^2 \,\mathrm{LAI}^2 U_h^2 + 2gh\frac{\theta_e - \hat{\theta}}{\hat{\theta}}}, \quad (1)$$

where γ is a constant (=0.277) depending on the horizontal wind and downward penetrating air parcel speed profiles below-canopy height h (e.g., Inoue, 1963; Amiro, 1990a; Poggi, Porporato, et al., 2004; Yi, 2008), $\hat{c}_d$ is the mean drag coefficient below h (equal to 0.15 for this study), LAI is leaf area index, U_h is horizontal

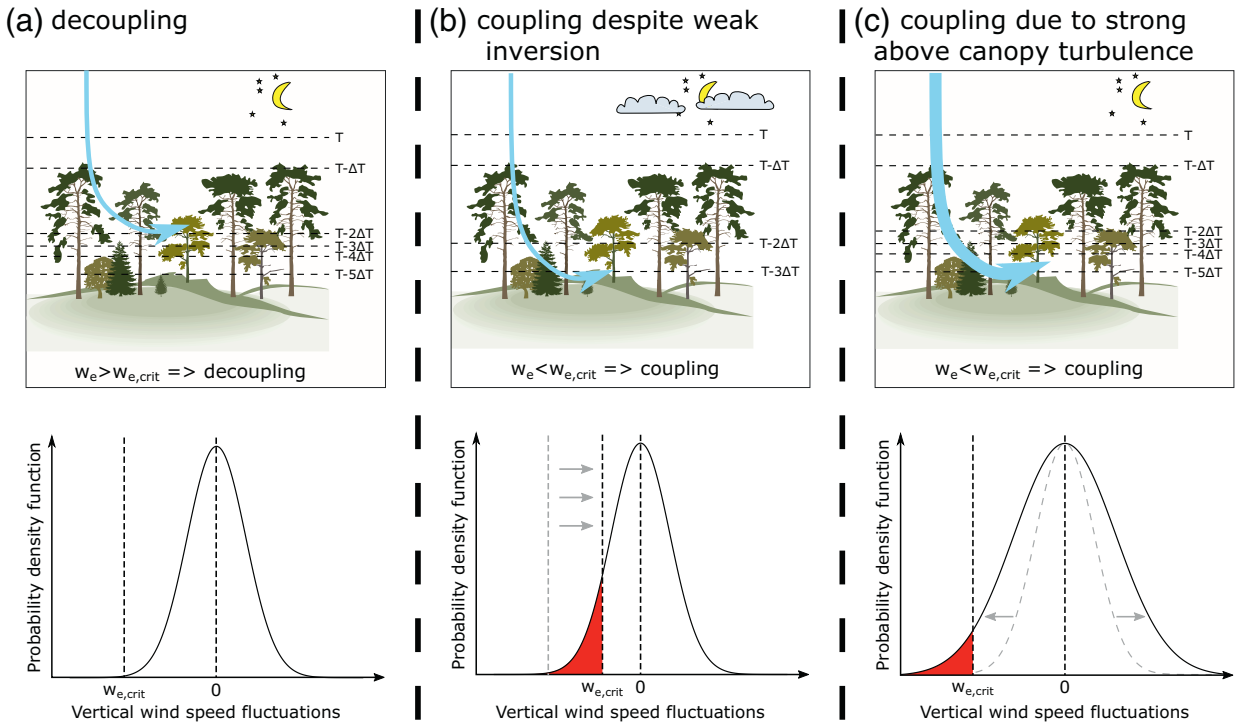

Figure 1. Schematic illustration of different decoupling situations. (a): the above-canopy flow is decoupled from the surface since the negative vertical wind speed fluctuations are not strong enough to counterbalance the movement hindering forces. (b): coupling with the surface due to weaker stratification compared to (a). (c): coupling due to stronger turbulent fluctuations when compared to (a). Bottom: fraction of w' data below $w_{e,\mathrm{crit}}$ is shown with red.

wind speed at the canopy height (m s^{-1}), g is the acceleration due to gravity (m s^{-2}), $\hat{\theta}$ is the mean potential temperature below h and θ_e is the potential temperature of the downward moving air parcel. If the speed of the air parcel is equal to $w_{e,\mathrm{crit}}$, then its kinetic energy is sufficient to counterbalance the work performed against the hindering forces. However, if it is less than this critical speed, then its downward movement stops before it reaches the ground and as a result interaction with the surface does not occur (see Figure 1).

In order to couple above-canopy flow with the forest floor, a large enough fraction of negative vertical wind speed fluctuations (w') needs to be below $w_{e,\mathrm{crit}}$. Considering Taylor's frozen turbulence hypothesis, this coincides with the definition that in coupled flow large enough cross-sectional area of the flow at height z needs to be governed by strong downward gusts which interact with the surface. Here we defined the flow to be coupled with the surface when more than 5% of the w' data were below $w_{e,\mathrm{crit}}$, weakly coupled when between 1% and 5% of w' data were below $w_{e,\mathrm{crit}}$ and decoupled when less than 1% were below $w_{e,\mathrm{crit}}$. Future work is needed to validate the general applicability of these thresholds, yet their applicability at two contrasting sites are demonstrated below (see also Section 4.4). Assuming Gaussian distribution for w', these criteria can be described using the standard deviation of w (σ_w):

$$0.43 \leq \begin{cases} \Omega & \geq 0.61 \rightarrow \text{coupled} \\ \Omega & < 0.61 \rightarrow \text{weaklycoupled} \\ \Omega & < 0.43 \rightarrow \text{decoupled} \end{cases} \quad (2)$$

where the decoupling metric Ω is defined as $\frac{\sigma_w}{|w_{e,crit}|}$. Therefore the flow can couple with the ground if σ_w increases (turbulent mixing increases), U_h or LAI decrease (canopy drag decreases) or $(\theta_e - \hat{\theta})$ or h decreases (influence of buoyancy and vertical distance decrease).

Atmospheric observations are typically made at some distance above the canopy during which the speed of downward propagating air parcel may be already slowed down due to stratification. The change in the speed of the air parcel when it traverses between heights z and h can be calculated as

$$w_e(z) = -\sqrt{w_e(h)^2 + 2g(z-h)\frac{\theta_e - \tilde{\theta}}{\tilde{\theta}}}, \tag{3}$$

where $w_e(z)$ and $w_e(h)$ are the air parcel speed at heights z and h and $\tilde{\theta}$ is the mean air potential temperature between z and h. Hence, in order to evaluate the coupling of air at height z with the ground, Equation 1 should be used to calculate $w_{e,\mathrm{crit}}$ at the canopy height (h) and then use Equation 3 to translate this value from h to z prior to comparing to σ_w values at height z.

In the case of neutral stratification, $w_{e,\mathrm{crit}}$ reduces to

$$w_{e,crit} = -2\gamma\,\hat{c}_d\,\mathrm{LAI}U_h, \tag{4}$$

indicating that the limiting vertical wind speed needed to couple with the forest floor increases linearly with LAI and U_h. On the other hand, in the case of flat surfaces without emergent vegetation (i.e., LAI ≈ 0), $w_{e,\mathrm{crit}}$ reduces to

$$w_{e,crit} = -\sqrt{2gz\frac{\theta_e - \hat{\theta}}{\hat{\theta}}} = -\sqrt{2}zN, \tag{5}$$

where N is the Brunt-Väisälä frequency estimated using the bulk θ gradient ($N = \sqrt{\frac{g(\theta_e - \hat{\theta})}{\hat{\theta}z}}$). Using the definition for buoyancy length scale ($L_B = \frac{\sigma_w}{N}$; Mahrt, 1979; Mahrt et al., 2012; Moum, 1996; Sorbjan, 2006; Sorbjan & Balsley, 2008) we can write

$$\Omega = \frac{L_B}{\sqrt{2}z}. \tag{6}$$

Hence, in the case of LAI ≈ 0, the criterium for the flow to couple with the surface (Equation 2) can be described with the ratio between L_B and height z.

3. Data and Instrumentation

Measurements were collected at two contrasting locations: observations at Hyytiälä boreal pine forest (61.845°N, 24.289°E, 181 m a.s.l) and during "Fluxes over snow-covered surfaces II" (FLOSS-II) campaign above snow-covered rangeland (40.659°N, 106.324°W, 2,477 m a.s.l). Hyytiälä is part of the Integrated Carbon Observation System (ICOS) measurement network (Franz et al., 2018) and has contributed to the global measurement network FLUXNET since the initiation of the site in 1996. The forest is governed by Scots pines (*Pinus sylvestris*) with approximate tree height of 17 m. One-sided LAI of the forest is 4 $m^2\ m^{-2}$ and the canopy layer is between 10 and 17 m. Turbulence profiles within the forest have been studied in Launiainen et al. (2007). In this study observations made during summer 2019 (May 25 to September 30) were utilized. The measurement configuration consisted of vertical fiber-optic based distributed temperature sensing (DTS) observations (until July 10), EC flux measurements (27 m height; Rebmann et al., 2018) and temperature and CO_2 concentration profiles (Montagnani et al., 2018). For details, see Peltola, Lapo, Martinkauppi et al. (2020a), however, there were four notable differences: (1) 10-min averaging period was used, (2) single-ended data (May 25 to June 3) were also included, (3) both directions in the double-ended configuration were utilized, and (4) the DTS temperature observations were denoised using singular value decomposition prior to analysis (Epps & Krivitzky, 2019). Note that denoizing has an effect only on Figure 2, since otherwise mean profiles were used. When calculating $w_{e,\mathrm{crit}}$, DTS measurements were utilized when available. All the data analyses were restricted to night-time periods (global radiation <5 W m^{-2}).

The observations made during the FLOSS-II measurement campaign (from December 2002 to end of March 2003) have been widely utilized in the analysis of vSBL (e.g., Mahrt, 2010; Mahrt & Vickers, 2005; Mahrt &

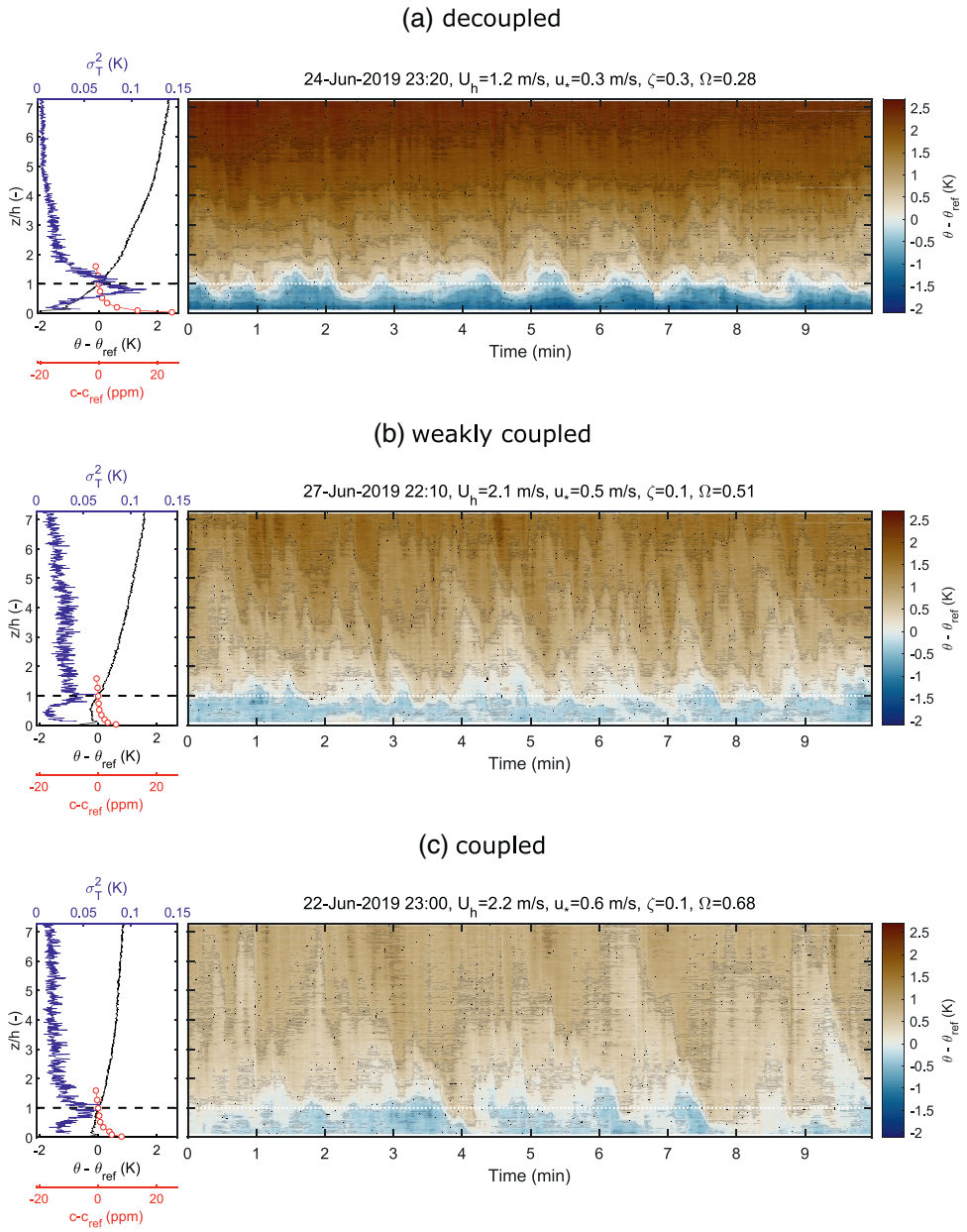

Figure 2. Right: examples of DTS temperature data during contrasting flow regimes (black lines = θ isolines). Left: corresponding temperature variance (blue), mean potential temperature (θ, black) and CO_2 concentration (c, red dots) profiles. c_{ref} and θ_{ref} equal mean c and θ values at canopy height (h). DTS, distributed temperature sensing.

Vickers, 2006; Sun et al., 2020). A 30 m tall tower located in a flat terrain with grass and partial snow-coverage was instrumented with three-dimensional sonic anemometers at seven levels and slow-response thermometers at eight levels. Quality-controlled and 5 min averaged data were retrieved from https://doi.org/10.5065/D6QC01XR (UCAR/NCAR – Earth Observing Laboratory, 2017).

4. Results and Discussion

4.1. Examples of Contrasting Flow Regimes

Figure 2 shows three 10-min examples of observations in the 125 m tall mast in Hyytiälä pine forest during contrasting flow regimes: (a) turbulent flow above-canopy which was decoupled from the forest floor,

(b) turbulent flow weakly coupled to the ground, and (c) strongly turbulent flow coupled to the ground. Coherent eddies consisting of sweep-ejection cycle (Finnigan et al., 2009; Thomas & Foken, 2007b) were observed in all of the examples, but only in (c) they were clearly coupled with the ground. The downward moving sweep phases of the coherent motions can be identified as the warm tongues penetrating into the cold below-canopy air space, whereas the ejections bring relatively cold below-canopy air to upper levels above the forest canopy (due to downward directed heat flux). Note that the sweeping phases in (a) did not reach the forest floor and as a result the flow was decoupled from the ground. This was identified also with the decoupling metric Ω (see subplot title).

CO_2 concentration profiles showed clear differences between the three examples, as a result from the different mixing regimes. The overall concentration difference between the highest (27 m) and lowest level (0.5 m) were 26, 7, and 9 ppm, respectively. Note that in case (a) this concentration difference resulted almost entirely from the CO_2 pooled below 8.8 m height, since the CO_2 above this height was effectively flushed out from the ecosystem by the coherent eddies.

4.2. Decoupling in Relation to TKE Production and Transport

Above open terrain, Sun et al. (2012) argued that in stably stratified coupled flow regime turbulent kinetic energy (TKE) should be bulk shear-driven (U/z) due to large eddies and shear production dominating the TKE budget. Hence, they analyzed V_{TKE} ($V_{\mathrm{TKE}} = \sqrt{\mathrm{TKE}} = \sqrt{\sigma_u^2 + 0.5\sigma_v^2 + 0.5\sigma_w^2}$) dependency on U and found a threshold value for U above which V_{TKE} dependency on U was linear. Observations falling in this strong wind regime have been considered to relate to coupled flow regime (Acevedo et al., 2016; Freundorfer et al., 2019; Lan et al., 2018; Mahrt et al., 2015; Sun et al., 2016). Figures 3a and 3b show V_{TKE} dependency on U for two heights in FLOSS-II dataset, with data differentiated to separate flow regimes (based on Equation 2) prior to analysis. In contrast to Sun et al. (2012), in the coupled regime no U threshold was observed and V_{TKE} followed the same linear dependence on U regardless of wind speed value. This suggests that in the stable coupled regime TKE was driven by bulk shear as proposed by Sun et al. (2012), however, this holds regardless of U not confirming the interpretation in Sun et al. (2012). Similar results were found for the forest site (Hyytiälä) using above-canopy U and V_{TKE} (not shown). Hence, we argue that flow decoupling cannot be judged based on U alone.

In prior studies, cross-canopy coupling have been analyzed by comparing concurrent measurements of σ_w below- and above-canopies (Freundorfer et al., 2019; Jocher et al., 2017, 2018; Thomas et al., 2013). Linear dependence between the two observations of σ_w were thought to signal coupling, since downward penetrating canopy-scale sweeps dominate the below-canopy TKE in coupled flow (Freundorfer et al., 2019; Russell et al., 2017; Vickers & Thomas, 2013). In accordance with these studies, the coupled flow regime was typically related to periods with high above-canopy V_{TKE} with a linear dependence between above- and below-canopy V_{TKE} (Figures 3c and 3d). In contrast, low above-canopy V_{TKE} was related to decoupled regime. In this regime, below-canopy TKE was dominated by Kármán vortex streets created behind trees and hence independent of above-canopy TKE (Cava et al., 2008; Russell et al., 2017) since downward propagating sweeps did not reach the below-canopy air space (see also Figure 2b). In our study, the wake-production generated a clear secondary peak in turbulence spectra (especially in 1 m height data) at the vortex shedding frequency based on constant Strouhal number, U and tree trunk diameter (not shown). At intermediate above-canopy V_{TKE} levels (0.5...0.8 m/s) the observations related to coupled flow regime departed from the linear dependence observed at higher V_{TKE} values. This might be due to importance of both, wake-production and sweeps, on below-canopy TKE at these above-canopy TKE levels and further analyses are warranted.

4.3. Turbulent Fluxes in the Coupled and Decoupled Layer

The sensible heat flux (H) profiles in the FLOSS-II dataset were analyzed in the view of flow decoupling dependency on height (Equation 6, Section 4.4.1). Nocturnal flux profiles were calculated so that each of the seven measurement heights was used as the highest observational level identified to be coupled with the surface (denoted with z_{co}). Hence, observations below and above z_{co} correspond to coupled and decoupled layers, respectively. The fluxes were normalized with the H values at height z_{co} (H_{co}). Below z_{co} nearly

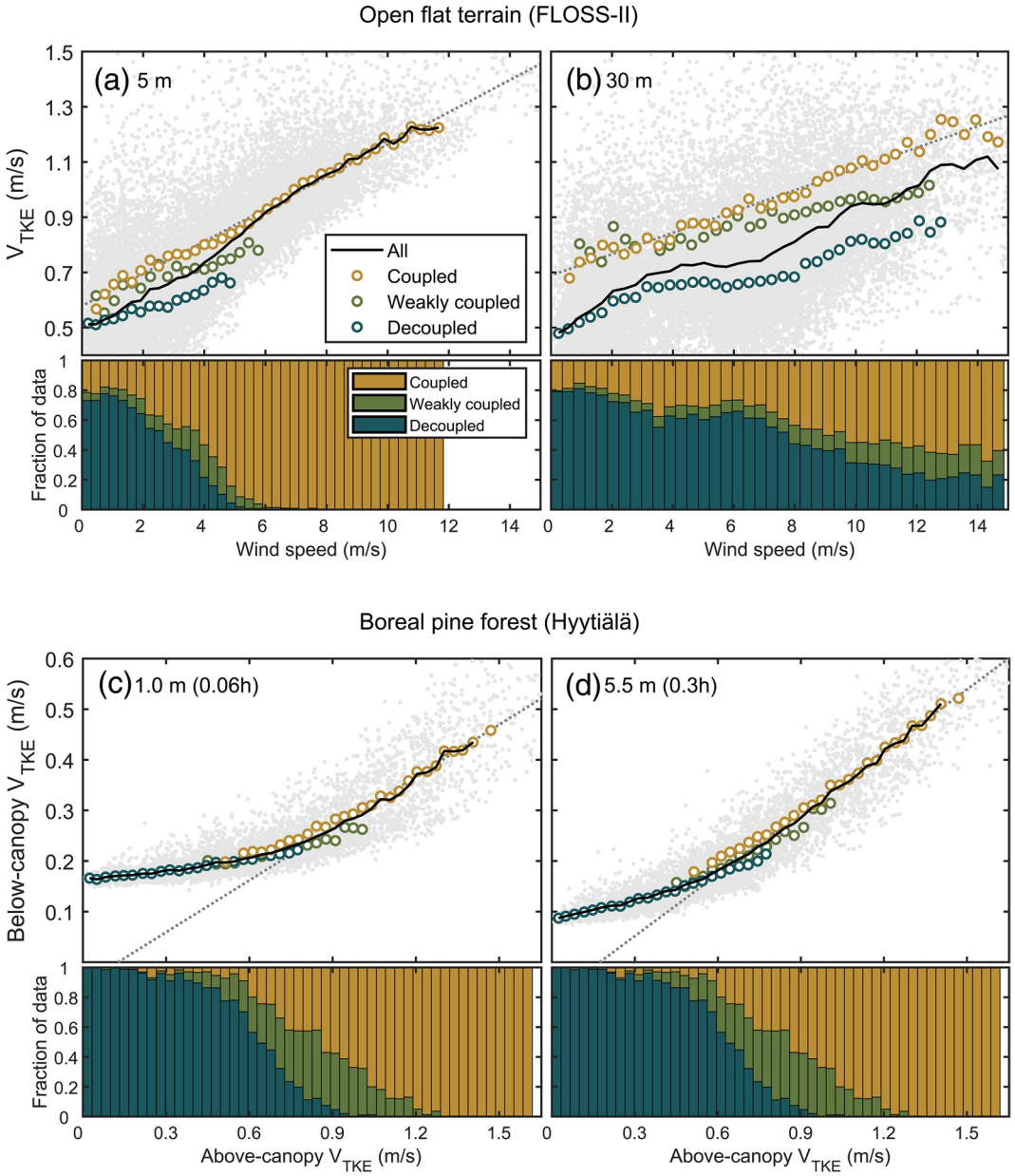

Figure 3. (a) and (b) V_{TKE} dependency on wind speed (U) at FLOSS-II following Sun et al. (2012). Additionally, data were divided into different coupling regimes (see Equation 2) prior to analysis. Note that threshold wind speed (Sun et al., 2012) was not observed in the coupled regime. (c) and (d) Comparison of above- and below-canopy V_{TKE} at Hyytiälä following Thomas et al. (2013). Gray dots = all the night-time data, circles and black lines = bin-averages for bins with more than 20 data points. Bottom: fraction of data in the three flow regimes (Equation 2). FLOSS-II, Fluxes over snow-covered surfaces II.

constant H was observed, whereas above z_{co} the flux H decreased with height, since the flow above z_{co} was not connected to the surface (Figure 4a). In the coupled air layer (i.e., below z_{co}), bin-averaged H was between $0.95H_{co}$ and $1.18H_{co}$ in agreement with the typical notion for constant-flux layer flows where the vertical turbulent fluxes are expected to vary by ±10%. Note that discrepancies between flux footprints at different heights and biases stemming from instrument calibrations may have also influenced the observed H profiles.

CO_2 fluxes measured above the Hyytiälä forest during night depended on the degree of coupling (i.e., Ω) when $\Omega < 0.61$, whereas in the coupled regime the fluxes were independent of Ω due to direct coupling of

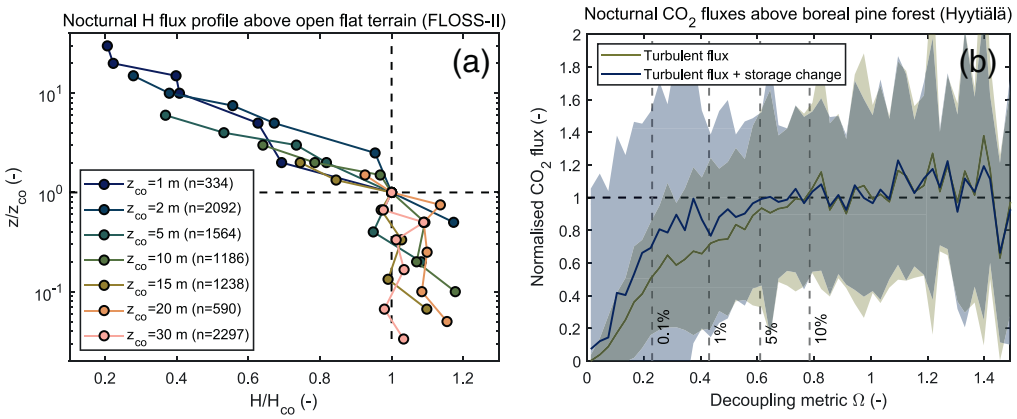

Figure 4. The physical interpretation of the coupling metric for (a) sensible heat profiles at FLOSS-II and (b) cross-canopy coupling of carbon dioxide at Hyytiälä. (a): Normalized sensible heat flux (H) profiles (bin medians) observed at FLOSS-II. Profiles were calculated from periods when height z_{co} was coupled with the surface (cf. Equation 2), but heights above z_{co} were not. Fluxes were normalized with H observed at z_{co} (H_{co}) (b): Normalized nocturnal CO_2 fluxes measured at Hyytiälä plotted against Ω (lines = bin means, areas = $\pm\sigma$). Data were filtered based on stationarity criteria (Foken & Wichura, 1996). The storage change term (Finnigan, 2006) was also included. Fluxes were normalized with 2-week running means of nocturnal CO_2 fluxes during coupled regime. Vertical dashed lines = fraction of w' data below $w_{e,crit}$. FLOSS-II, Fluxes over snow-covered surfaces II.

flux measurement height with the ground with turbulent mixing being no longer limiting. Figures 4a and 4b show physically the same phenomenon, but for different sites. Fluxes above z_{co} (Figure 4a) and during periods with $\Omega < 0.61$ (Figure 4b) correspond to decoupled flow, whereas on the contrary above z_{co} and during periods with $\Omega \geq 0.61$ correspond to coupled flow.

These results suggest that the method proposed in Section 2 can be used to estimate the depth of the layer that was coupled with the surface and hence, for example, to assess whether the observed turbulent fluxes related to the exchange of heat (FLOSS-II) or CO_2 (Hyytiälä) on the surface. Note that these results were obtained at two contrasting measurement sites without site-specific thresholds. This is due to using a ratio of variables related to kinetic energy (σ_w) and the energy required to couple with the ground ($w_{e,crit}$) in the analysis, instead of using σ_w (Acevedo et al., 2009; Jocher et al., 2018; Thomas et al., 2013) or related variables (u_*, U; e.g., Gu et al., 2005; Sun et al., 2012) alone. Furthermore, this ratio does not depend on the source for the turbulent mixing in any way, it merely compares the existing kinetic energy to the energy needed to couple with the ground. Hence the decoupling metric should be applicable also in situations when the source does not conform with the traditional boundary layer (e.g., upside down boundary layer; Mahrt, 2014; Mahrt et al., 2013).

4.4. Controls on Flow Decoupling

4.4.1. Flows Above Short Vegetation

Above short vegetation (i.e., LAI ≈ 0), $w_{e,crit}$ depends linearly on z and N (Equation 5) and the definition for coupling (Equation 2) can be written as

$$\sigma_w \geq 0.61\sqrt{2}zN. \tag{7}$$

Hence, at a given value for N, the σ_w needed to couple the flow with the surface increases linearly with height. This is in line with prior experimental findings (Acevedo et al., 2016; Mahrt et al., 2013). The increase reflects the fact that the kinetic energy of downward moving air parcel needs to be higher when the height increases since there is a thicker air column below the air parcel within which the buoyancy force opposes its movement, that is, the potential energy of the air parcel increases with height. In the FLOSS-II dataset, rarely the upper level was identified to be coupled with the surface when the observation level below was not (less than 1% of observations). In general, the lower levels were observed to be coupled with

the surface more frequently than the upper levels, for instance 5 m height was coupled with the surface 64% of time, whereas 20 m height only 39% of time.

4.4.2. Flows Above Tall Vegetation

In the case of neutral stratification below-canopy height, using Equation 4 the definition for coupling (Equation 2) can be written as

$$I_w \geq 1.22\gamma\,\hat{c}_d\,\mathrm{LAI}, \tag{8}$$

where I_w is the vertical turbulence intensity at the canopy height $\left(I_w = \frac{\sigma_w}{U_h}\right)$. Note the similarity between the right hand side of Equation 8 and the ratio between canopy height and coherent eddy penetration depth in Cava et al. (2008), Ghisalberti (2009), and Nepf et al. (2007) (i.e., $\propto \hat{c}_d\mathrm{LAI}$) which describes whether the coherent canopy eddies are interacting with the surface or not. At the Hyytiälä site in near-neutral conditions above the forest I_w was on average 0.26, whereas the limit for decoupling calculated using Equation 8 was 0.20, indicating coupling at this site in near-neutral conditions. In contrast, Thomas et al. (2013) observed frequent decoupling above their dense forest (LAI = 9.4 $\mathrm{m^2 m^{-2}}$) even during daytime despite similar I_w levels (0.25–0.30) and the decoupling could have been predicted with Equation 8. It should be noted however that γ and $\hat{c}_d$ depend on canopy architecture (Amiro, 1990a, 1990b) and the influence of these parameters should be investigated. Clearly this method should be tested across range of sites with contrasting canopies, albeit similarities to the studies of Cava et al. (2008), Ghisalberti (2009), and Nepf et al. (2007) do suggest of a more general applicability.

5. Conclusions

Poor understanding of the vSBL is an obstacle for all scientific studies investigating surface-atmosphere interactions, in particular in the case of canopy flows. Here, we propose a novel simple first-principle based scheme to identify periods when the air flow is not in interaction with the underlying surface (i.e., it is decoupled). It was shown to correctly identify periods when the measured turbulent fluxes were not representative of the fluxes at the surface. The metric for flow decoupling based on this concept enabled analytical derivation of flow decoupling dependency on height, stratification and leaf area index. The approach is an improvement to the commonly used methods based on the example, friction velocity filtering, since (1) the proposed approach takes into account also changes in forces hindering the coupling (canopy drag, stable stratification) unlike traditional methods which utilize metrics for turbulent mixing or production alone and (2) it is based on first principles and not on ad hoc empirical correlations. From a practical point-of-view, the approach requires only basic micrometeorological measurements (turbulence measurements at one height and temperature profile below it) in addition to knowledge of canopy density and hence should be applicable at most flux sites through the complete gradient from locations with short canopies to dense tall forests.

Data Availability Statement

FLOSS-II data can be acquired at https://doi.org/10.5065/D6QC01XR and Hyytiälä data at https://doi.org/10.5281/zenodo.4250443 (Peltola, Lapo, & Thomas, 2020b).

Acknowledgments
FLOSS-II data were provided by NCAR/EOL under the sponsorship of the National Science Foundation (https://data.eol.ucar.edu/). University of Helsinki, in particular Timo Vesala and technical staff at the Hyytiälä research station, are acknowledged for enabling the measurement campaign in Hyytiälä. O. Peltola is supported by the postdoctoral researcher project (decision 315424) funded by the Academy of Finland. K. Lapo and C. K. Thomas received funding from the European Research Council (ERC) under the European Union's Horizon 2020 research and innovation program (grant agreement No 724629, project DarkMix).

References

Acevedo, O. C., Mahrt, L., Puhales, F. S., Costa, F. D., Medeiros, L. E., & Degrazia, G. A. (2016). Contrasting structures between the decoupled and coupled states of the stable boundary layer. *Quarterly Journal of the Royal Meteorological Society*, *142*(695), 693–702. https://doi.org/10.1002/qj.2693

Acevedo, O. C., Moraes, O. L. L., Degrazia, G. A., Fitzjarrald, D. R., Manzi, A. O., & Campos, J. G. (2009). Is friction velocity the most appropriate scale for correcting nocturnal carbon dioxide fluxes? *Agricultural and Forest Meteorology*, *149*(1), 1–10. https://doi.org/10.1016/j.agrformet.2008.06.014

Amiro, B. D. (1990a). Comparison of turbulence statistics within three boreal forest canopies. *Boundary-Layer Meteorology*, *51*(1), 99–121. https://doi.org/10.1007/BF00120463

Amiro, B. D. (1990b). Drag coefficients and turbulence spectra within three boreal forest canopies. *Boundary-Layer Meteorology*, *52*(3), 227–246. https://doi.org/10.1007/BF00122088

Aubinet, M., Feigenwinter, C., Heinesch, B., Bernhofer, C., Canepa, E., Lindroth, A., et al. (2010). Direct advection measurements do not help to solve the night-time CO_2 closure problem: Evidence from three different forests. *Agricultural and Forest Meteorology*, *150*(5), 655–664. https://doi.org/10.1016/j.agrformet.2010.01.016

Baldocchi, D. (2014). Measuring fluxes of trace gases and energy between ecosystems and the atmosphere – the state and future of the eddy covariance method. *Global Change Biology*, *20*(12), 3600–3609. https://doi.org/10.1111/gcb.12649

Cava, D., Katul, G. G., Sempreviva, A. M., Giostra, U., & Scrimieri, A. (2008). On the anomalous behavior of scalar flux – variance similarity functions within the canopy sub-layer of a dense alpine forest. *Boundary-Layer Meteorology*, *128*(1), 33. https://doi.org/10.1007/s10546-008-9276-z

Cescatti, A., & Marcolla, B. (2004). Drag coefficient and turbulence intensity in conifer canopies. *Agricultural and Forest Meteorology*, *121*(3), 197–206. https://doi.org/10.1016/j.agrformet.2003.08.028

Epps, B. P., & Krivitzky, E. M. (2019). Singular value decomposition of noisy data: Noise filtering. *Experiments in Fluids*, *60*(8), 126. https://doi.org/10.1007/s00348-019-2768-4

Finnigan, J. (2000). Turbulence in plant canopies. *Annual Review of Fluid Mechanics*, *32*(1), 519–571. https://doi.org/10.1146/annurev.fluid.32.1.519

Finnigan, J. (2006). The storage term in eddy flux calculations. *Agricultural and Forest Meteorology*, *136*(3–4), 108–113. https://doi.org/10.1016/j.agrformet.2004.12.010

Finnigan, J., Shaw, R. H., & Patton, E. G. (2009). Turbulence structure above a vegetation canopy. *Journal of Fluid Mechanics*, *637*, 387–424. https://doi.org/10.1017/S0022112009990589

Foken, T., & Wichura, B. (1996). Tools for quality assessment of surface-based flux measurements. *Agricultural and Forest Meteorology*, *78*(1–2), 83–105.

Franz, D., Acosta, M., Altimir, N., Arriga, N., Arrouays, D., Aubinet, M., et al. (2018). Toward long-term standardised carbon and greenhouse gas observations for monitoring Europe's terrestrial ecosystems: A review. *International Agrophysics*, *32*(4). https://doi.org/10.1515/intag-2017-0039

Freundorfer, A., Rehberg, I., Law, B. E., & Thomas, C. (2019). Forest wind regimes and their implications on cross-canopy coupling. *Agricultural and Forest Meteorology*, *279*, 107696. https://doi.org/10.1016/j.agrformet.2019.107696

Friedlingstein, P., Jones, M. W., O'Sullivan, M., Andrew, R. M., Hauck, J., Peters, G. P., et al. (2019). Global carbon budget 2019. *Earth System Science Data*, *11*(4), 1783–1838. https://doi.org/10.5194/essd-11-1783-2019

Ghisalberti, M. (2009). Obstructed shear flows: Similarities across systems and scales. *Journal of Fluid Mechanics*, *641*, 51–61. https://doi.org/10.1017/S0022112009992175

Grachev, A. A., Andreas, E. L., Fairall, C. W., Guest, P. S., & Persson, P. O. G. (2013). The critical Richardson number and limits of applicability of local similarity theory in the stable boundary layer. *Boundary-Layer Meteorology*, *147*(1), 51–82. https://doi.org/10.1007/s10546-012-9771-0

Gu, L., Falge, E. M., Boden, T., Baldocchi, D. D., Black, T. A., Saleska, S. R., et al. (2005). Objective threshold determination for nighttime eddy flux filtering. *Agricultural and Forest Meteorology*, *128*(3), 179–197. https://doi.org/10.1016/j.agrformet.2004.11.006

Inoue, E. (1963). On the turbulent structure of airflow within crop canopies. *Journal of the Meteorological Society of Japan. Ser. II*, *41*(6), 317–326. https://doi.org/10.2151/jmsj1923.41.6_317

Jocher, G., Marshall, J., Nilsson, M. B., Linder, S., De Simon, G., Hörnlund, T., et al. (2018). Impact of canopy decoupling and subcanopy advection on the annual carbon balance of a boreal scots pine forest as derived from eddy covariance. *Journal of Geophysical Research: Biogeosciences*, *123*(2), 303–325. https://doi.org/10.1002/2017JG003988

Jocher, G., Ottosson Löfvenius, M., De Simon, G., Hörnlund, T., Linder, S., Lundmark, T., et al. (2017). Apparent winter CO_2 uptake by a boreal forest due to decoupling. *Agricultural and Forest Meteorology*, *232*, 23–34. https://doi.org/10.1016/j.agrformet.2016.08.002

Kruijt, B., Malhi, Y., Lloyd, J., Norbre, A. D., Miranda, A. C., Pereira, M. G. P., et al. (2000). Turbulence statistics above and within two Amazon rain forest canopies. *Boundary-Layer Meteorology*, *94*(2), 297–331. https://doi.org/10.1023/A:1002401829007

Lan, C., Liu, H., Li, D., Katul, G. G., & Finn, D. (2018). Distinct turbulence structures in stably stratified boundary layers with weak and strong surface shear. *Journal of Geophysical Research: Atmosphere*, *123*(15), 7839–7854. https://doi.org/10.1029/2018JD028628

Launiainen, S., Vesala, T., Mölder, M., Mammarella, I., Smolander, S., Rannik, L., et al. (2007). Vertical variability and effect of stability on turbulence characteristics down to the floor of a pine forest. *Tellus B: Chemical and Physical Meteorology*, *59*(5), 919–936. https://doi.org/10.1111/j.1600-0889.2007.00313.x

Li, D., Salesky, S. T., & Banerjee, T. (2016). Connections between the Ozmidov scale and mean velocity profile in stably stratified atmospheric surface layers. *Journal of Fluid Mechanics*, *797*. https://doi.org/10.1017/jfm.2016.311

Mahrt, L. (1979). Penetrative convection at the top of a growing boundary layer. *Quarterly Journal of the Royal Meteorological Society*, *4105*(444), 469–485. https://doi.org/10.1002/qj.49710544411

Mahrt, L. (2010). Variability and maintenance of turbulence in the very stable boundary layer. *Boundary-Layer Meteorology*, *135*(1), 1–18. https://doi.org/10.1007/s10546-009-9463-6

Mahrt, L. (2014). Stably stratified atmospheric boundary layers. *Annual Review of Fluid Mechanics*, *46*(1), 23–45. https://doi.org/10.1146/annurev-fluid-010313-141354

Mahrt, L., Richardson, S., Seaman, N., & Stauffer, D. (2012). Turbulence in the nocturnal boundary layer with light and variable winds. *Quarterly Journal of the Royal Meteorological Society*, *138*(667), 1430–1439. https://doi.org/10.1002/qj.1884

Mahrt, L., Sun, J., Blumen, W., Delany, T., & Oncley, S. (1998). Nocturnal boundary-layer regimes. *Boundary-Layer Meteorology*, *88*(2), 255–278

Mahrt, L., Sun, J., & Stauffer, D. (2015). Dependence of turbulent velocities on wind speed and stratification. *Boundary-Layer Meteorology*, *155*(1), 55–71. https://doi.org/10.1007/s10546-014-9992-5

Mahrt, L., Thomas, C., Richardson, S., Seaman, N., Stauffer, D., & Zeeman, M. (2013). Non-stationary generation of weak turbulence for very stable and weak-wind conditions. *Boundary-Layer Meteorology*, *147*(2), 179–199. https://doi.org/10.1007/s10546-012-9782-x

Mahrt, L., Thomas, C. K., Grachev, A. A., & Persson, P. O. G. (2018). Near-surface vertical flux divergence in the stable boundary layer. *Boundary-Layer Meteorology*, *169*(3), 373–393. https://doi.org/10.1007/s10546-018-0379-x

Mahrt, L., & Vickers, D. (2005). Boundary-layer adjustment over small-scale changes of surface heat flux. *Boundary-Layer Meteorology*, *116*(2), 313–330. https://doi.org/10.1007/s10546-004-1669-z

Mahrt, L., & Vickers, D. (2006). Extremely weak mixing in stable conditions. *Boundary-Layer Meteorology*, *119*(1), 19–39. https://doi.org/10.1007/s10546-005-9017-5

Montagnani, L., Grünwald, T., Kowalski, A., Mammarella, I., Merbold, L., Metzger, S., et al. (2018). Estimating the storage term in eddy covariance measurements: The ICOS methodology. *International Agrophysics*, *32*(4), 551–567. https://doi.org/10.1515/intag-2017-0037

Moum, J. N. (1996). Energy-containing scales of turbulence in the ocean thermocline. *Journal of Geophysical Research*, *6101*(C6), 14095–14109. https://doi.org/10.1029/96JC00507

Nepf, H., Ghisalberti, M., White, B., & Murphy, E. (2007). Retention time and dispersion associated with submerged aquatic canopies. *Water Resources Research*, *443*(4). https://doi.org/10.1029/2006WR005362

Nieuwstadt, F. T. M. (1984). The turbulent structure of the stable, nocturnal boundary layer. *Journal of the Atmospheric Sciences*, *41*(14), 2202–2216. https://doi.org/10.1175/1520-0469(1984)041⟨2202:TTSOTS⟩2.0.CO;2

Peltola, O., Lapo, K., Martinkauppi, I., O'Connor, E., Thomas, C. K., & Vesala, T. (2020a). Suitability of fiber-optic distributed temperature sensing to reveal mixing processes and higher-order moments at the forest-air interface. *Atmospheric Measurement Techniques Discussions*, 1–31. https://doi.org/10.5194/amt-2020-260

Peltola, O., Lapo, K., & Thomas, C. (2020b). *Dataset for "A physics-based universal indicator for vertical decoupling and mixing across canopies architectures and dynamic stabilities"*. https://doi.org/10.1002/essoar.10504742.1

Poggi, D., Katul, G. G., & Albertson, J. D. (2004a). Momentum transfer and turbulent kinetic energy budgets within a dense model canopy. *Boundary-Layer Meteorology*, *111*(3), 589–614. https://doi.org/10.1023/B:BOUN.0000016502.52590.af

Poggi, D., Porporato, A., Ridolfi, L., Albertson, J. D., & Katul, G. G. (2004b). The effect of vegetation density on canopy sub-layer turbulence. *Boundary-Layer Meteorology*, *111*(3), 565–587. https://doi.org/10.1023/B:BOUN.0000016576.05621.73

Raupach, M. R., Finnigan, J. J., & Brunei, Y. (1996). Coherent eddies and turbulence in vegetation canopies: The mixing-layer analogy. *Boundary-Layer Meteorology*, *78*(3), 351–382. https://doi.org/10.1007/BF00120941

Rebmann, C., Aubinet, M., Schmid, H., Arriga, N., Aurela, M., Burba, G., et al. (2018). ICOS eddy covariance flux-station site setup: A review. *International Agrophysics*, *32*(4), 471–494. https://doi.org/10.1515/intag-2017-0044

Russell, E. S., Liu, H., & Lamb, B. (2017). Wavelet spectra within a forest subcanopy under different wind directions and stabilities. *Journal of Geophysical Research: Atmosphere*, *122*(16), 8399–8409. https://doi.org/10.1002/2017JD026817

Santana, R. A., Dias-Júnior, C. Q., da Silva, J. T., Fuentes, J. D., do Vale, R. S., Alves, E. G., et al. (2018). Air turbulence characteristics at multiple sites in and above the Amazon rainforest canopy. *Agricultural and Forest Meteorology*, *260–261*, 41–54. https://doi.org/10.1016/j.agrformet.2018.05.027

Sorbjan, Z. (2006). Local structure of turbulence in stably stratified boundary layers. *Journal of the Atmospheric Sciences*, *63*(5), 1526–1537. https://doi.org/10.1175/JAS3704.1

Sorbjan, Z., & Balsley, B. B. (2008). Microstructure of turbulence in the stably stratified boundary layer. *Boundary-Layer Meteorology*, *129*(2), 191–210. https://doi.org/10.1007/s10546-008-9310-1

Sun, J., Lenschow, D. H., LeMone, M. A., & Mahrt, L. (2016). The role of large-coherent-eddy transport in the atmospheric surface layer based on CASES-99 observations. *Boundary-Layer Meteorology*, *160*(1), 83–111. https://doi.org/10.1007/s10546-016-0134-0

Sun, J., Mahrt, L., Banta, R. M., & Pichugina, Y. L. (2012). Turbulence regimes and turbulence intermittency in the stable boundary layer during CASES-99. *Journal of the Atmospheric Sciences*, *69*(1), 338–351. https://doi.org/10.1175/JAS-D-11-082.1

Sun, J., Takle, E. S., & Acevedo, O. C. (2020). Understanding physical processes represented by the Monin–Obukhov bulk formula for momentum transfer. *Boundary-Layer Meteorology*, *177*, 69–95. https://doi.org/10.1007/s10546-020-00546-5

Thomas, C., & Foken, T. (2007a). Flux contribution of coherent structures and its implications for the exchange of energy and matter in a tall spruce canopy. *Boundary-Layer Meteorology*, *123*(2), 317–337. https://doi.org/10.1007/s10546-006-9144-7

Thomas, C., & Foken, T. (2007b). Organized motion in a tall spruce canopy: Temporal scales, structure spacing and terrain effects. *Boundary-Layer Meteorology*, *122*(1), 123–147. https://doi.org/10.1007/s10546-006-9087-z

Thomas, C., Martin, J. G., Law, B. E., & Davis, K. (2013). Toward biologically meaningful net carbon exchange estimates for tall, dense canopies: Multi-level eddy covariance observations and canopy coupling regimes in a mature Douglas-fir forest in Oregon. *Agricultural and Forest Meteorology*, *173*, 14–27. https://doi.org/10.1016/j.agrformet.2013.01.001

UCAR/NCAR – Earth Observing Laboratory. (2017). *NCAR/EOL 5 minute quality controlled ISFF data, Version 1.0*. UCAR/NCAR – Earth Observing Laboratory. https://doi.org/10.5065/D6QC01XR

Vickers, D., & Thomas, C. K. (2013). Some aspects of the turbulence kinetic energy and fluxes above and beneath a tall open pine forest canopy. *Agricultural and Forest Meteorology*, *181*, 143–151. https://doi.org/10.1016/j.agrformet.2013.07.014

Watanabe, T. (2004). Large-eddy simulation of coherent turbulence structures associated with scalar ramps over plant canopies. *Boundary-Layer Meteorology*, *112*(2), 307–341. https://doi.org/10.1023/B:BOUN.0000027912.84492.54

Williams, A. G., Chambers, S., & Griffiths, A. (2013). Bulk mixing and decoupling of the nocturnal stable boundary layer characterized using a ubiquitous natural tracer. *Boundary-Layer Meteorology*, *149*(3), 381–402. https://doi.org/10.1007/s10546-013-9849-3

Yi, C. (2008). Momentum transfer within canopies. *Journal of Applied Meteorology and Climatology*, *47*(1), 262–275. https://doi.org/10.1175/2007JAMC1667.1

Zeeman, M. J., Eugster, W., & Thomas, C. K. (2013). Concurrency of coherent structures and conditionally sampled daytime sub-canopy respiration. *Boundary-Layer Meteorology*, *146*(1), 1–15. https://doi.org/10.1007/s10546-012-9745-2